Original Article

Institution of MECHANICAL ENGINEERS
Journal of MECHANICAL ENGINEERING SCIENCE

Proc IMechE Part C:
J Mechanical Engineering Science
0(0) 1–16

DOI: 10.1177/0954406215581692
pic.sagepub.com
SAGE

On the choice of initial clearance and prediction of leakage flow rate for a rotating gas turbine seal

Sivakumar Subramanian[1], AS Sekhar[1] and BVSSS Prasad[2]

Abstract

The present work proposes a design procedure along with guidelines for the choice of initial clearance of a typical rotating gas turbine seal in a secondary air system. The basis for the design is to prevent seal rubbing against stator, by ensuring that the centrifugal and thermal growths of the seal are within the safe operating limits. As a case study, a six-tooth straight-through rotating labyrinth seal configuration is considered with wide ranging seal parameters, namely the seal inner radius (25–700 mm), speed (1000–5000 rad/s), temperature (200–650 °C) and pressure ratio (1.1–2.5). By means of an iterative process, which involves computational fluid dynamics and finite element analysis techniques, and with a choice of initial clearance, an extensive database is generated. The results are presented in terms of non-dimensional variables, namely seal clearance ratio, centrifugal growth ratio, thermal growth ratio, operating clearance ratio due to centrifugal growth and operating clearance ratio due to thermal growth. It is found that the value of clearance ratio depends significantly on the dimensionless radial position. For a seal clearance ratio of 0.01, at 3000 rad/s, the leakage flow rate gets reduced by 18 and 4%, respectively for pressure ratios of 1.1 and 2.5, when the centrifugal growth alone is considered. When both centrifugal and thermal growths are considered, the percentage reduction becomes about 70% for the same seal operating at 3000 rad/s and 204 °C, and it is as high as 95% at 426 °C.

Keywords

Gas turbine seal, initial clearance, design, seal rubbing, centrifugal growth, thermal growth, leakage, computational fluid dynamics, finite element analysis

Date received: 25 September 2014; accepted: 5 March 2015

Introduction

The importance of efficient sealing towards safe and reliable operation of a modern gas turbine (GT) engine need not be overemphasized, for there are as many as 50 sealing locations in a typical secondary air system of a GT engine.[1] Seals help in reducing air leakage and provide control over the secondary air for cooling the critical components in a predesigned manner. When the engine is in operation, the seals are subjected to mechanical loads due to high rate of rotation and thermal loads due to elevated temperatures. Thus, they are prone to experience both centrifugal and thermal deformations predominantly in the radial direction. As the radial growth of the rotating seals is dependent on their linear speed and thermal conditions, they experience distinctly different radial growths when placed at different radial locations. Thus, the operating clearance values of the seals could be substantially different from the initial (assembly/design) seal clearances.

Several alternate methods are discussed in the literature[1–7] to estimate the leakage flow from the secondary air system as a basis for the seal design. They are (a) analytical, e.g. bulk-flow model (b), experimental using static/rotating seal rig at ambient/hot conditions, and (c) numerical, e.g. using CFD codes. Besides, displacement sensors have been commonly used to measure seal operating clearances. More often, the centrifugal radial growth is estimated by the Roark's formula[8] and the thermal growth by the linear relation for thermal expansion.[9] Even recent studies like Li et al.,[10] Subramanian et al.,[11] Anderson,[12] and Qiu et al.[13] quoted these formulae for estimating the radial growth. Further, the leakage characteristics of the seals are estimated using modified St. Venant's equation with empirical constants

[1]Machine Design Section, Department of Mechanical Engineering, Indian Institute of Technology Madras, Chennai, India
[2]Thermal Turbomachines Laboratory, Department of Mechanical Engineering, Indian Institute of Technology Madras, Chennai, India

Corresponding author:
AS Sekhar, Department of Mechanical Engineering, Indian Institute of Technology Madras, Chennai 600036, India.
Email: as_sekhar@iitm.ac.in

determined from experiments. As the seal clearance value explicitly appears in this equation, the leakage can easily be estimated from the combination of, say, the Roark's, linear thermal expansion and modified St. Venant's formulae. This is the method followed by most researchers[8,9,12] irrespective of the type of seal, be it a traditional straight-through labyrinth seal or advanced pocket damper seal (PDS). Gamal et al.[8] have accounted for the centrifugal growth of plain solid shaft using Roark's formula while testing PDS, with static teeth. Li et al.[10] have estimated the centrifugal growth using a finite element (FE) model for the prediction of leakage flow of PDS. They have concluded that for a rotational speed of 60,200 r/min, typically, the seal clearance of the PDS is reduced by 6.2 and 9.2% with finite element analysis (FEA) and the Roark's formula, respectively. However, both had ignored thermal growth owing to the low test temperature range (10–17 °C). Li et al.[14] have reported the centrifugal growth using a FE model for the prediction of leakage flow of a hybrid labyrinth brush seal. However, no comparison with any analytical model has been reported. Further, they also have neglected the thermal growth as the temperature is confined to 40 °C. A recent study by Subramanian et al.[11] takes into account radial growth (both centrifugal and thermal) in calculating the actual leakage flow rate for a rotating labyrinth seal. They have provided quantitative information, perhaps for the first time, on the centrifugal and thermal growth values and their influence on leakage flow rates for a wide range of operating conditions. The radial growths predicted using FEA and rotating flat disk analytical model are compared qualitatively. Recently, Qiu et al.[13] carried out detailed investigations into the flow behaviour of multi-stage brush seals for three operating clearances (labyrinths: 0.2–0.4 mm; brush: 0.0–0.2 mm) and four rotational speeds. The leakage rate is numerically predicted using Reynolds Averaged Navier–Stokes (RANS) equations coupled with non-Darcian porous medium approach. They take into account the rotor centrifugal growth in brush seal flow calculations to predict the seal leakage more accurately using Roark's formula, similar to the one used by Subramanian et al.[11] Further, they have compared the FEA results of Li et al.[14] with their analytical results and find that their analytical predictions are almost equal to FEM results. Thus, there are only a very few studies reported on the determination of the radial growth of the seals and the associated leakage characteristics.

There is no clear mention about the choice of initial (design) clearance in the available literature. For instance, Hwang et al.[3] have developed labyrinth seals operating with 25 μm of radial clearance per 25 mm of seal diameter for engine secondary flow. They have reported that the seals could perform satisfactorily up to speed of 11,500 r/min (surface speed = 225 m/s), differential pressure of 6.8 bar and temperature up to 535 °C. However, it appears that their design is based on some rule of thumb rather than a systematic approach. Alexiou and Mathioudakis[15] have reported the modelling aspects of typical secondary air system components, including seals, but no consideration is given to the initial clearance and the seal deformation towards their engine performance simulations. Studies by Amirante et al.[16] and Ganine et al.[17] have taken the stator/rotor deflection pertaining to a particular flight cycle into account, but the centrifugal and thermal growth values are not presented and no information is provided on the choice of seal clearance. Hence, there is a need for understanding the choice of initial clearance for different seal locations, and the subsequent operating clearance due to both centrifugal and thermal growth of rotating GT seals, especially under elevated operating conditions. In order to predict the radial growth, operating clearance and leakage flow rate of a typical rotating seal, a combined computational fluid dynamics (CFD) and FE methodology had been established and reported by the authors in their previous work.[11] The centrifugal and thermal growths predicted by FE model for two different configurations, namely fix-fix end conditions and fix-free end conditions were compared with analytical models, based on rotating flat disk formulation. It is found that the FEA results corresponding to the fix-free end condition are closer to the analytical calculations and are used for further investigations with the flow analysis to study the influence of radial growth on leakage.

The present work is therefore an attempt to relate the leakage flow characteristics with the radial growth of a rotating GT seal for different radial positions based on the conventional computational tools, thereby arriving at the right initial clearance for the desired location and operating conditions. Further, fix-free edge condition is investigated, which is akin to the actual physical configurations in a typical aero-engine and the same methodology is adopted to give an insight into the choice of initial clearance and to predict radial growth and the subsequent operating clearance and leakage for various seal inner radius and operating conditions. It may be pointed out that the initial clearance (C) is the radial gap (see Figure 1) between the outer radius of the seal and stator housing, under static cold condition.

Non-dimensional design variables

As the seal may be placed at any radial location in the system, and subjected to specific mechanical and thermal loadings, its radial growth and the resulting net operating clearance will be distinctly different. Primarily, the centrifugal growth (U_{CG}) is a function of rotational speed and radius, and thermal growth (U_{TG}) is a function of temperature and radius. Before the seal is placed at a particular location, the initial

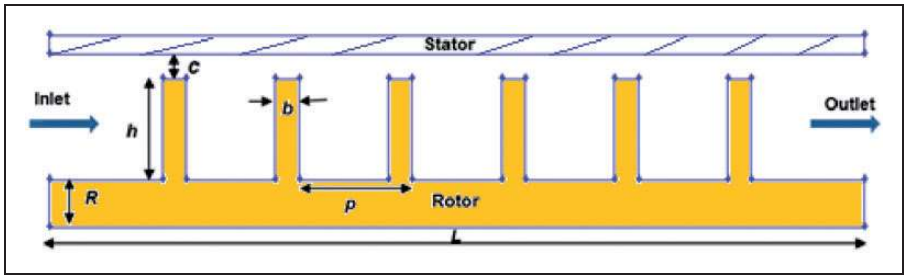

Figure 1. Schematic of GT seal (not to scale).

clearance is thus an important design variable to avoid potential rubbing and ensure a safe operation. In this context, seven non-dimensional design variables representing centrifugal growth, thermal growth and operating clearance values are defined as follows

$$\text{Seal clearance ratio: } SCR = \frac{C}{R} \tag{1}$$

$$\text{Centrifugal growth ratio: } CGR = \frac{U_{CG}}{C} \tag{2}$$

With the reduced operating clearance due to CG alone: $C_1 = C - U_{CG}$

$$\text{Operating clearance ratio due to } CG \text{ alone: } OCRC = \frac{C_1}{C} \tag{3}$$

$$\text{Thermal growth ratio: } TGR = \frac{U_{TG}}{C} \tag{4}$$

With the reduced operating clearance due to TG alone: $C_2 = C - U_{TG}$

$$\text{Operating clearance ratio due to } TG\text{: } OCRT = \frac{C_2}{C} \tag{5}$$

$$\text{Net radial growth ratio: } NRGR = \frac{U_{CG} + U_{TG}}{C} \tag{6}$$

With the net reduced operating clearance due to net radial growth: $C_3 = C - (U_{CG} + U_{TG})$

$$\text{Net operating clearance ratio due to } CG \text{ and } TG\text{: } NOCR = \frac{C_3}{C} \tag{7}$$

For a given initial clearance and the desired radial position of interest, the radial growth and the consequent operating clearance can be obtained from the corresponding design charts (as an example, design charts are provided in 'Results and discussion' section for the seal considered). These charts also give an insight on the operating speed and temperature limits and aid in arriving at an optimum initial clearance. A generic design procedure is provided in 'Design guidelines and procedure' section, which describes the application of an iterative process involving CFD and FEA techniques and the formulated non-dimensional design variables to decide on the choice of initial clearance.

Table 1. Geometrical parameters and operating conditions.

L = Length of the seal (mm)	86.5
p = Pitch of the seal (mm)	12
b = Width of the seal tooth (mm)	2.5
h = Height of the seal tooth (mm)	10.5
n = Number of teeth	6
R = Inner radius of the seal (mm)	25–700
C = Initial clearance of the seal (mm)	0.1–2.5
ω = Rotational speed of the seal (rad/s)	0–5000
T = Fluid temperature (°C)	27–650
PR = Pressure ratio	1.1–2.5

Case study: Seal considered and operating conditions

A six-tooth straight-through rotating labyrinth seal configuration is considered to demonstrate the generic design procedure outlined in 'Design guidelines and procedure' section. Figure 1 shows the physical model of the seal chosen[11] for the present work.

The geometrical details and operating conditions of the seal considered are furnished in Table 1. The ranges are chosen so as to simulate the GT engine conditions as well as to facilitate comparison and arriving at some useful conclusions. In the present study, the seal locations are represented by means of varying the seal inner radius representing the different radial positions of the seal from the shaft axis.

Validation

FE modelling

In the present work, the FE-based radial growth prediction for fix-free edge conditions is reported for a

wide range of rotational speed and temperature at the preferred locations. Although the radial growth of the GT seal is generally of the order of μm, it plays a very significant role because it is of the same order as the clearance. Thus, they strongly affect the leakage flow characteristics of seal, hence it is crucial to estimate the radial growth accurately. A comprehensive 3D FEA is carried out employing ANSYS Mechanical 14.

The rotor comprising of a solid shaft/disk along with the labyrinth seal teeth mounted across the edge of the shaft is modelled collectively as a rotating flat disk of uniform thickness. The radial deformation due to rotation and high temperature is considered independently. A full 3D model of the rotor is computationally demanding. Noting the symmetry of both the geometry and loading conditions, a 45° 3D sector model of the rotor is considered. Symmetry conditions are imposed on the sector end faces. In the present FE model, X, Y and Z axis represents the axial, radial and circumferential direction of the seal, respectively. The origin is located at the left end of the axis (X-axis) of the seal. Figure 2 depicts the typical FE mesh consisting of 85,995 elements which is used for the rotor with an inner radius of 350 mm. Detailed element insensitivity and grid independency analysis were carried out and reported in Subramanian et al.[11] Accordingly, SOLID185,[18] a 3D, eight-node structural solid element is chosen for the present analysis. The element has three degrees of freedom, viz. translations along the nodal X, Y and Z directions. In addition, rotations along the nodal X, Y and Z directions have been added. The sparse direct solver has been chosen along with the mass matrix formulation being set to default. The accuracy of the sector model is ensured by comparing the results of full 3D model for a rotor configuration with seal inner radius of 50 mm. A typical comparison of centrifugal growth results obtained for full 3D model and 45° 3D sector model at a rotational speed of 1000 rad/s is shown in Figure 3.

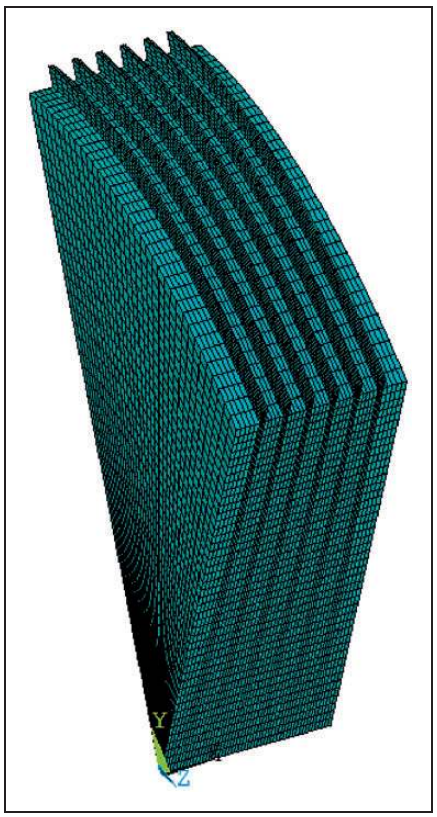

Figure 2. Three-dimensional FE mesh for rotor: $R = 350$ mm.

For the prediction of centrifugal growth, the linear and isotropic assumptions are made and the stiffness of the material is defined in terms of Young's modulus. Density and Poisson's ratio values are provided. The properties[19] of Inconel 718, a Ni-based super alloy are used for the rotor material at a room temperature of 21 °C as provided in Table 2. For representing fix-free edge condition, both axial and torsional constraints are imposed for the centre-line nodes, so as to avoid axial movement and twisting.

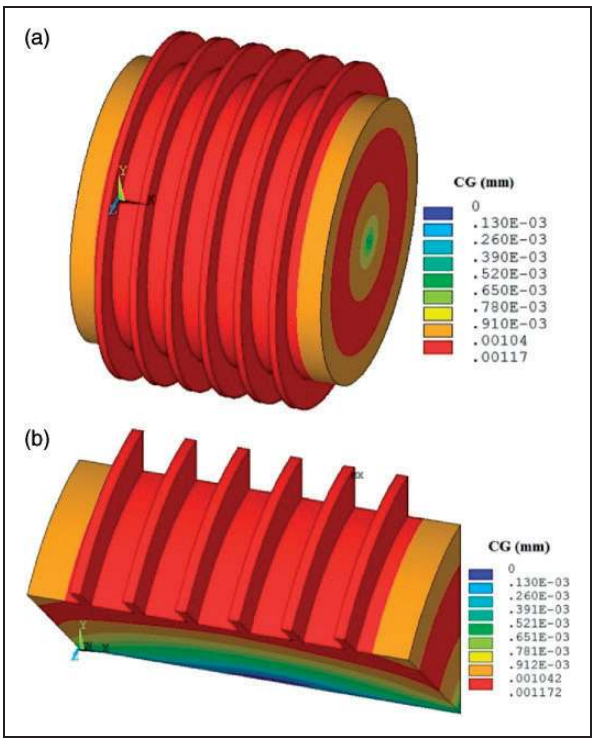

Figure 3. *CG* at $\omega = 1000$ rad/s for rotor $R = 50$ mm: (a) full 3D model (b) 45° sector model.

Table 2. Properties of rotor material: Inconel 718.

Property	Value
E = Modulus of elasticity (GPa)	200
N = Poisson's ratio	0.294
ρ = Density (kg/m^3)	8221
T_{ref} = Reference temperature (°C)	21

In other words, both translation and rotation along the nodal X direction are suppressed. In addition, translations along the nodal Y and Z directions are suppressed for the centre-line end nodes to mimic bearing effect. Rotation is defined along the X-axis with the angular speeds of interest, which are basically inertia loads that were applied for the entire rotor model.

Thermal modelling of the rotor is the most difficult owing to the temperatures on the upstream and downstream surfaces of the rotor being different and the heat transfer. It is assumed that the temperature throughout the thickness of the rotor surface is constant and equal to the fluid temperature. Further, it is assumed that there is no generation/transfer of heat. Thus, for the thermal growth prediction, a uniform fluid temperature value is applied for the entire rotor model. The solid–fluid temperature difference is varied parametrically in the present case. However, in practice, the values depend on the application. These assumptions give a conservative estimate of thermal growth, which eventually prevent rubbing and facilitate safe operation. It may be noted that the fix-free edge constraints are imposed as represented earlier, wherein both translation and rotation along the nodal direction suppressed for the centre-line nodes plus the translations along the nodal Y and Z directions are suppressed for centre-line end nodes. The temperature-dependent properties[19] of Inconel 718 for the corresponding surface temperature of the rotor are given in Table 3.

Table 3. Temperature-dependent properties of rotor material: Inconel 718.

T_s (°C)	E (GPa)	ν	$\alpha \times 10^{-6}$ (1/°C)
204	190	0.280	13.5
315	184	0.272	13.9
426	178	0.271	14.4
537	171	0.271	14.4
648	167	0.283	15.1

Timoshenko rotating flat disk (of uniform thickness) model[20,21] has been utilized to validate the present FE model quantitatively. The centrifugal and thermal growths are expressed in equations (8) and (10)

$$U_{CG} = \frac{\rho\omega^2(R+h)^3(1-\nu)}{4E} \tag{8}$$

where

$$\omega = \frac{2\pi N}{60} \tag{9}$$

$$U_{TG} = \alpha(R+h)(T_s - T_{ref}) \tag{10}$$

Figure 4 shows the comparison between FEA and analytical model for radial growth predictions as a function of speed and temperature for a rotor configuration with seal inner radius of 50 mm. It can be inferred that the centrifugal growth varies as a quadratic function with rotational speed. On the other hand, thermal growth varies almost linearly with temperature. Further, it is interesting to note that the thermal growth values are one order of magnitude higher than the centrifugal growth values for the chosen range of operating conditions. It is observed that the analytical model overpredicts the centrifugal

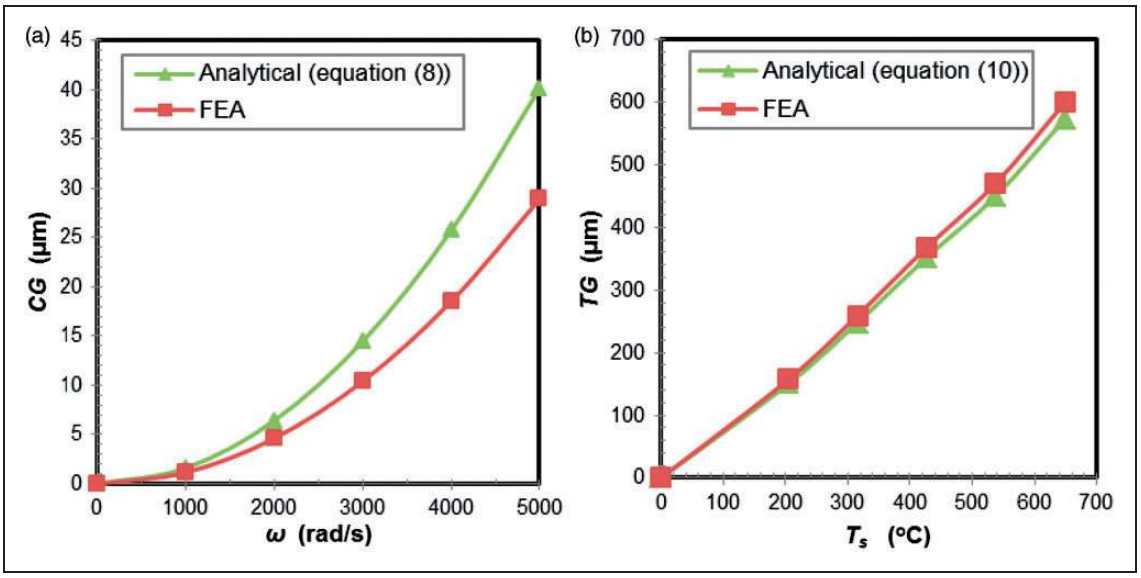

Figure 4. FEA versus analytical-based radial growth prediction for $R = 50$ mm (fix-free edge conditions) as a function of (a) speed (b) temperature.

growth by 28% and underpredicts the thermal growth by 5%, irrespective of angular speeds and temperature conditions. However, as the rotor radius is increased, the deviation is less than 10%. For instance, a rotor radius of 350 mm, the centrifugal growth experienced at an angular speed of 1000 rad/s is found to be 32 μm using FEA and 34 μm using analytical model (deviation being 6%). For the same rotor, the thermal growth experienced at a temperature of 204 °C is found to be 900 μm using FEA and 896 μm using analytical model (deviation being 1%). Thus, the comparisons between 3D FE and analytical model are satisfactory. The variation stated by the theory and the present numerical results is expected because of the 1D assumption in the theory rather than the uncertainty of the present results. Moreover, as the FEA analysis is carried out with well-tested commercial code ANSYS Mechanical 14, the rigor and reliability of the calculation is ensured.

Further, the robustness of the analytical model can be examined by comparisons with FEA results reported by Li et al.[14] for similar boundary conditions (fix-free edge condition). One of the labyrinth brush seals tested by them has a shaft radius of 335.5 mm, outer seal radius of 340 mm and clearance of 0.2 mm for an angular speed of 3000 r/min. The rotating flat disk model predicts the centrifugal growth as 26.21 μm, which is reasonably closer to the FEA results[14] (25 μm). Nevertheless, the analytical model has to be assessed for various rotor sizes, which needs further studies and presently is under investigation.

CFD modelling

The rotor spinning within the tight clearance gap (~0.1 mm) and the lack of flow symmetry makes the present problem 3D in nature. The 3D computational domain essentially comprises of inlet, outlet, rotor wall and stator wall. The seal length is extended by 20 mm at both the inlet and outlet region in order to ensure that boundary conditions do not have an undesirable effect on leakage flow through the seal. A 3D multi-block structured grid is created using ANSYS ICEM CFD 14. The fluid is air; the flow is steady, incompressible and turbulent. The initial air temperature is assumed equal to 300 K. Three-dimensional RANS equations are solved together with the additional transport equations for the turbulent kinetic energy and the turbulent dissipation rate, employing a commercial code ANSYS FLUENT 14. A Standard k–ε model, with enhanced wall treatment has been incorporated into the analysis. The present CFD methodology is already validated[11] against the 2D CFD analysis results reported by Kim and Cha[22] for a clearance of 2.5 mm. Further, the viability of the chosen turbulence model is ensured (see Figure 5) by comparing the present CFD results with the static rig results reported by Wittig et al.[23] for the same conditions. It can be inferred from Figure 5 that the present 3D CFD model (standard k–ε model, with enhanced wall treatment) predictions match reasonably well and closer to the experiment.[23] The detailed description of this problem and its numerical treatment were clearly discussed[11] for the seal configuration with inner radius of 50 mm and for an initial seal clearance of 0.5 mm. Similar treatment is extended for the same configuration with an initial clearance of 0.1, 1.5 and 2.5 mm. The details are not repeated for the sake of brevity.

A detailed grid independence analysis, similar to that reported by Hirano et al.[24] is carried out to ensure the adequacy of grid towards a reliable solution. Accordingly, the optimal number of divisions along the longitudinal and circumferential directions is arrived at first, followed by the lateral direction. Adequate care has been taken for placing the required nodes into the finer clearance gap without compromising on grid quality metrics. A typical grid independence study made for the seal configuration with inner radius 50 mm and clearance 0.1 mm is presented in Figure 6 for a pressure ratio (PR) of 1.1 and

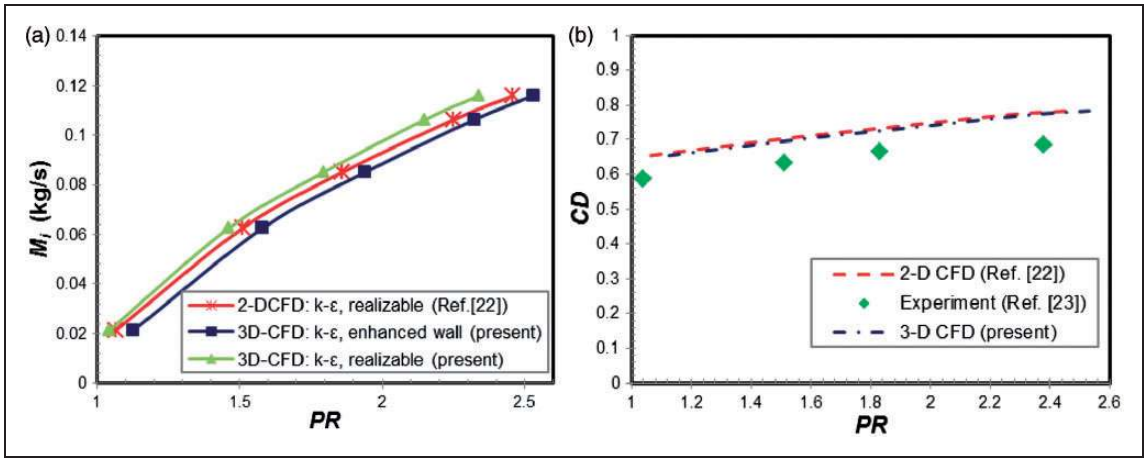

Figure 5. CFD model validation: (a) with other numerical models, (b) with experiment.

rotational speed of 1000 rad/s, under ambient condition. The number of nodes in the clearance gap is varied from two to five in increments of one; four nodes are found to be adequate to predict the leakage flow. Thus, the optimum grid size is about 0.97 million nodes for the seal configuration with inner radius 50 mm and clearance 0.1 mm. A typical CFD grid for the seal configuration with inner radius of 50 mm and for an initial seal clearance of 0.5 mm is provided in Subramanian et al.[11]

Results and discussion

The detailed centrifugal and thermal growth of a six-tooth rotating labyrinth GT seal estimated for the operating conditions of interest is presented in terms of dimensionless variables for fix-free edge conditions. The flow analysis for both initial clearances and operating clearances and the corresponding leakage flow rate are reported. In addition, the combined radial growth influence on leakage is investigated for a specified initial clearance of 0.5 mm and seal inner radius of 50 mm.

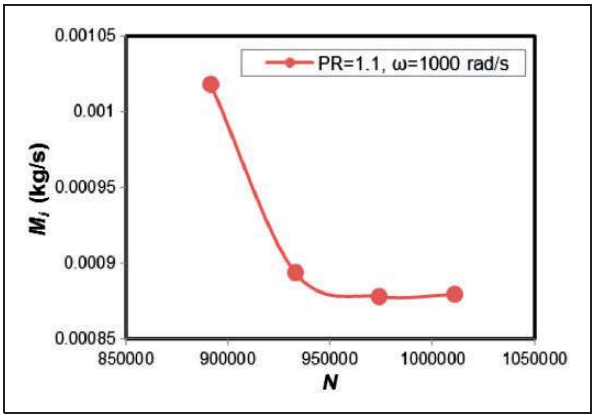

Figure 6. CFD grid independence study for $R = 50$ mm and $C = 0.1$ mm.

Non-dimensional centrifugal growths and operating clearances

Figures 7 through 10 depict the non-dimensional centrifugal growth and the resulting operating clearance as a function of seal inner radius for a constant initial clearance of 0.1, 0.5, 1.5 and 2.5 mm, respectively. These charts have been generated using the centrifugal growth predicted by FEA along with equations (1) to (3). The abscissa represents the seal clearance ratio (*SCR*) and the ordinate represents the non-dimensional centrifugal growth or the corresponding operating clearance. The centrifugal growth ratio (*CGR*) and the operating clearance ratio due to centrifugal growth (*OCRC*) (ranging from 0 to 1) along the ordinate denotes the magnitude of centrifugal growth and operating clearance. Whenever *CGR* approaches the higher bound '1' or *OCRC* approaches the lower bound '0', rubbing occurs. In order to prevent rubbing, a limiting *CGR* and *OCRC* have to be established for a particular temperature of interest so that a safe operating clearance (say ~0.1 mm) can be maintained.

It can be observed from Figure 7 that for a constant initial clearance of 0.1 mm, the *CGR* decreases with increasing *SCR*. As the rotational speed increases, the trend shifts progressively towards the right side and slightly above the lower speed line.

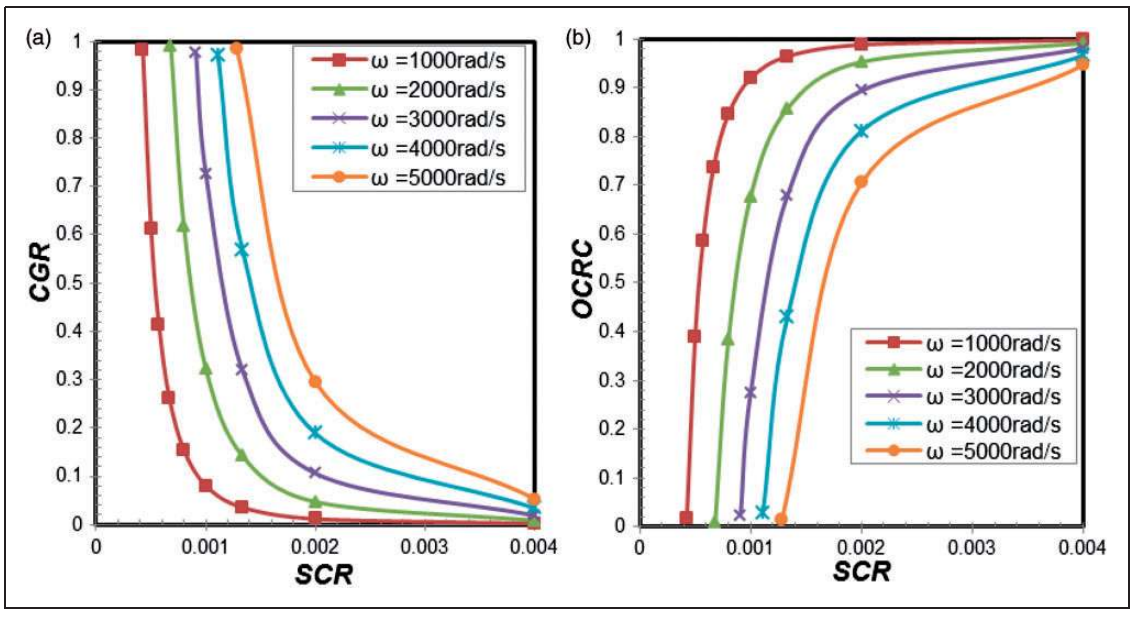

Figure 7. Non-dimensional (a) centrifugal growth and (b) operating clearance as a function of seal inner radius for an initial clearance of 0.1 mm at different angular speeds.

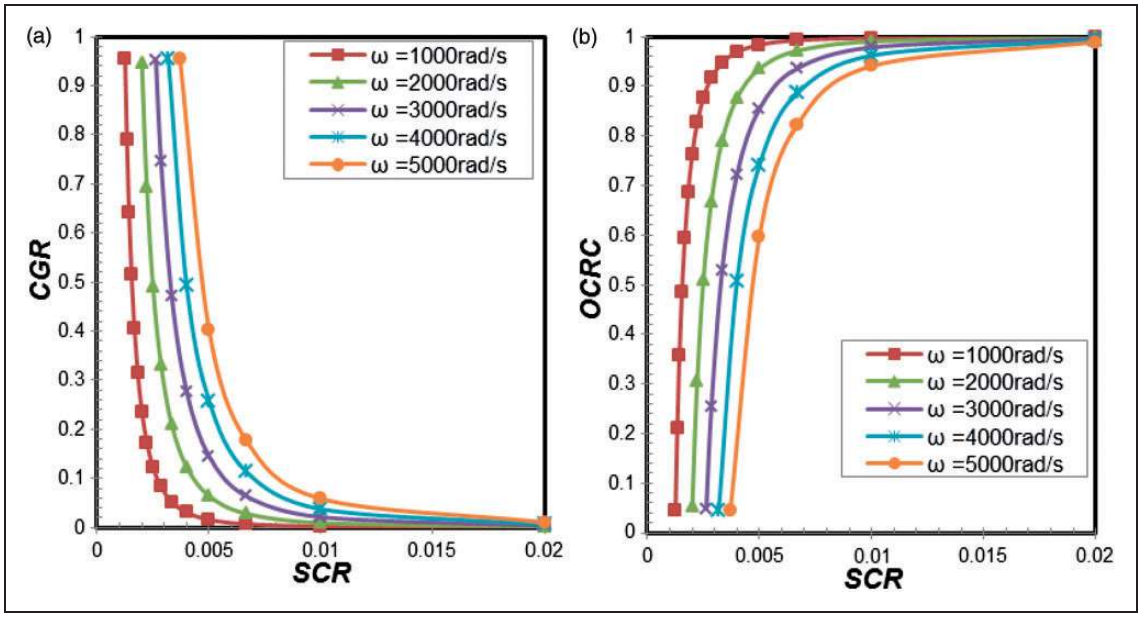

Figure 8. Non-dimensional (a) centrifugal growth and (b) operating clearance as a function of seal inner radius for an initial clearance of 0.5 mm at different angular speeds.

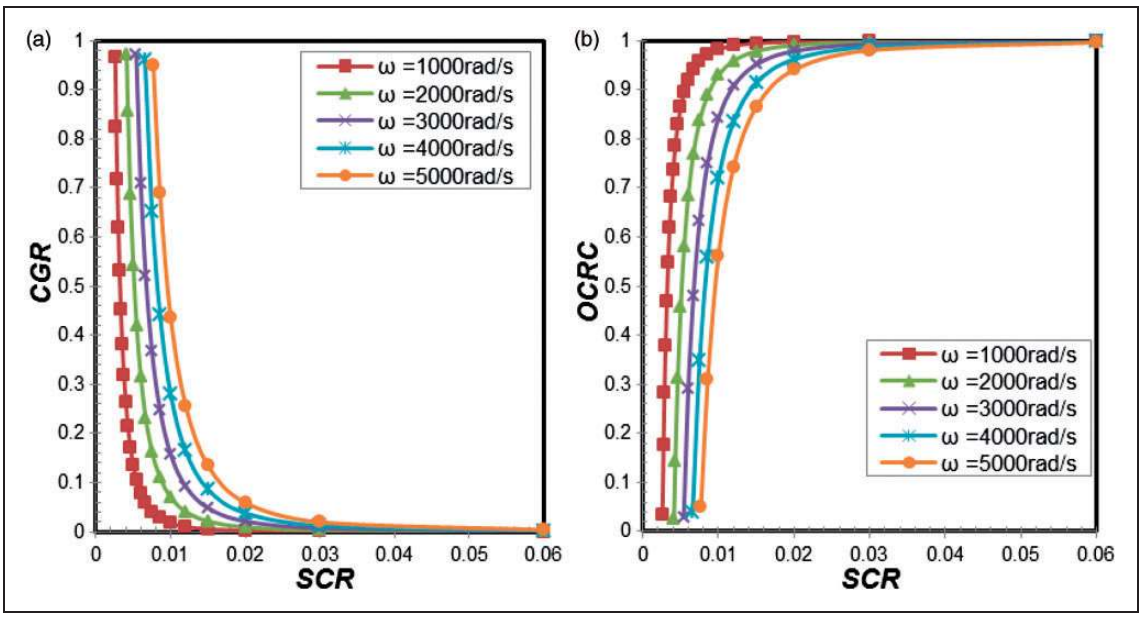

Figure 9. Non-dimensional (a) centrifugal growth and (b) operating clearance as a function of seal inner radius for an initial clearance of 1.5 mm at different angular speeds.

This implies that seals with smaller inner radius have a wide range of operating speed for a given initial clearance. In other words, the seals kept radially closer to the shaft axis have the maximum limiting speed and the farthest seal will have the minimum limiting speed. For instance, a seal with inner radius of 50 mm has a *CG* value of 1.2, 4.6, 10.4, 18.5 and 29 μm, respectively for $\omega = 1000$, 2000, 3000, 4000 and 5000 rad/s. In contrast, seal with a relatively large inner radius of 100 mm has a *CG* value of 7.8, 31.5, 70.5 μm, respectively for $\omega = 1000$, 2000 and 3000 rad/s. Thus for the same initial clearance of 0.1 mm, the maximum limiting speed is as high as 5000 rad/s for a smaller inner radius seal (50 mm) and it is restricted to as low as 3000 rad/s for the larger inner radius seal (100 mm). Further, it is interesting to note that the seal inner radius can approximately go up to 235, 145, 110, 90 and 75 mm for a seal operating at 1000, 2000, 3000, 4000 and 5000 rad/s, respectively. The foregoing results indicate that the radial position of the seal is limited by the rotational speed for a given initial clearance. It is evident from Figures 8 to 10 that as the clearance increases, the same trend of *CGR* decreasing with increasing *SCR* continues. Typically, *SCR* range

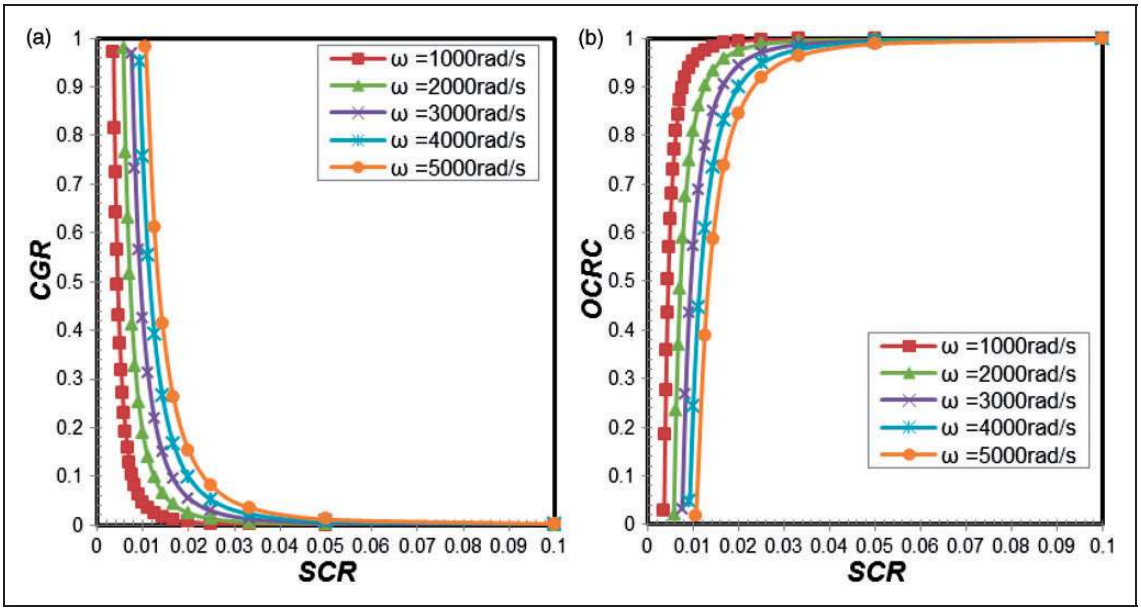

Figure 10. Non-dimensional (a) centrifugal growth and (b) operating clearance as a function of seal inner radius for an initial clearance of 2.5 mm at different angular speeds.

goes up to 0.004, 0.02, 0.06 and 0.1 for an initial clearance of 0.1, 0.5, 1.5 and 2.5 mm, respectively, for the chosen range of seal inner radii. Further, it is inferred that for a lower rotational speed (say 1000 rad/s), the seal inner radius up to 235, 400, 580 and 690 mm can be accommodated, respectively, for an initial clearance of 0.1, 0.5, 1.5 and 2.5 mm. For a higher rotational speed (say 5000 rad/s), the seal inner radius up to 75, 135, 195 and 235 mm can be covered, respectively, for the equivalent initial clearances.

It may be concluded from Figures 7 to 10 that *CG* is sensitive to the smaller *SCR*, irrespective of speed, ω and the influence decreases drastically, as *SCR* approaches 0.004, 0.01, 0.02 and 0.025, respectively, for the initial clearance of 0.1, 0.5, 1.5 and 2.5 mm. This implies that the influence of centrifugal growth on leakage can be anticipated to be insignificant beyond these limits. Thus, it is obvious that the centrifugal growth is more prominent at smaller clearance and higher rotational speed combinations. The foregoing discussion shows that for larger initial clearance, a broader range of seal inner radii can be accommodated, besides a wider operating speed range. However, the seal initial clearance can be ascertained only after determining the leakage flow rates, which is discussed in 'Leakage flow analysis' section.

Non-dimensional thermal growths and operating clearances

Figures 11 through 14 depict the non-dimensional thermal growth and the resulting operating clearance as a function of seal inner radius for a constant initial clearance of 0.1, 0.5, 1.5 and 2.5 mm, respectively. These charts have been generated using the thermal growth predicted by FEA along with equations (1), (4) and (5). The abscissa represents the *SCR* and the ordinate denotes the non-dimensional thermal growth or the corresponding operating clearance. The thermal growth ratio *(TGR)* and the operating clearance ratio due to thermal growth *(OCRT)* (ranging from 0 to 1) along the ordinate denote the magnitude of thermal growth and operating clearance. Whenever *TGR* approach the higher bound '1' or *OCRT* approach the lower bound '0', rubbing occurs. In order to prevent rubbing, a limiting *TGR* and *OCRT* have to be established for a particular rotational speed of interest so that a safe operating clearance (say ~0.1 mm) can be maintained.

In general, *TG* values are relatively higher than *CG* values for the chosen operating conditions of interest. However, the trends are almost the same as discussed earlier for *CG* charts. That is the *TGR* decreases with increasing *SCR* for a given initial clearance. As the temperature increases, the same trend shifts progressively more towards the right side and significantly more (than the *CG* trend shift towards right gradually and slightly above the lower speed line) above the lower temperature line proportionately. The reason being *TG* values are larger than *CG* values. Thus, the seals kept radially closer to the shaft axis have the maximum limiting temperature and the farthest seal will have the minimum limiting temperature. For instance, a seal with inner radius of 50 mm has a *TG* of 157, 259, 368, 470 and 599 μm, respectively, for temperatures of 204, 315, 426, 537 and 648 °C. In contrast, seal with a relatively large inner radius of 100 mm has a *TG* value of 272, 449, 637, 814 and 1037 μm, respectively, for the equivalent temperatures. It may be pointed out that for an initial clearance of 0.1 mm, even with no rotation, the seal cannot be operated for both the chosen range of seal inner

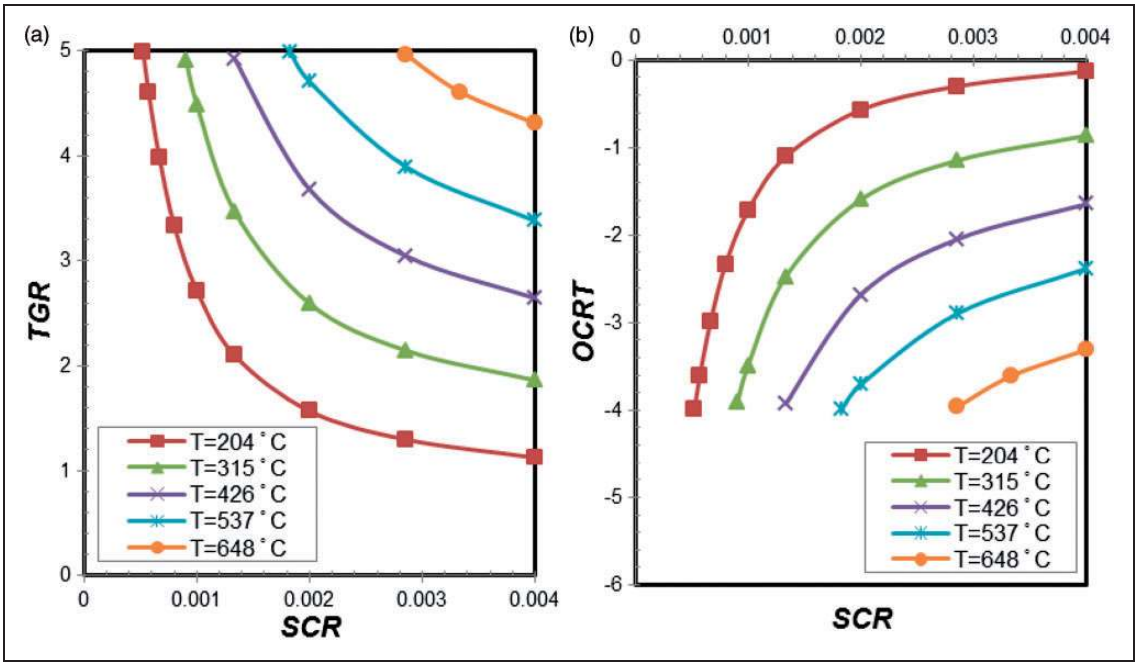

Figure 11. Non-dimensional (a) thermal growth and (b) operating clearance as a function of seal inner radius for an initial clearance of 0.1 mm at different temperature conditions.

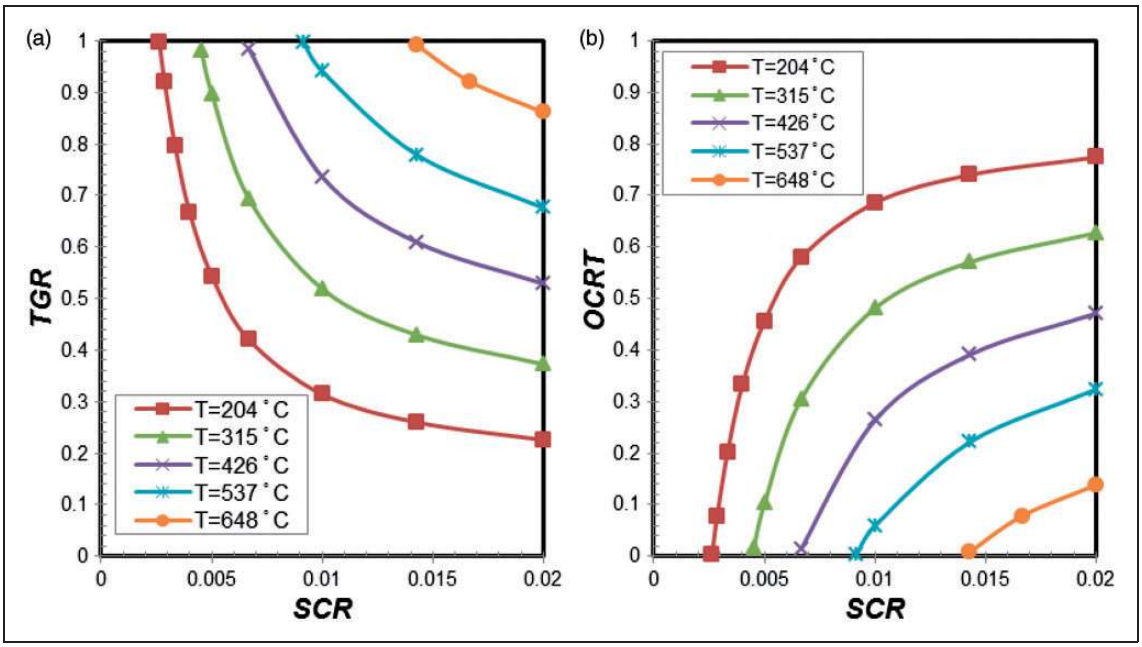

Figure 12. Non-dimensional (a) thermal growth and (b) operating clearance as a function of seal inner radius for an initial clearance of 0.5 mm at different temperature conditions.

radii and temperature conditions. Thus, the charts (Figure 11(a) and (b)) for the initial clearance of 0.1 mm are provided only to highlight this feature.

It can be inferred from Figure 12 that for a typical initial clearance of 0.5 mm, the seal inner radius can approximately go up to 190, 110, 75, 50 and 35 mm for a seal operating at 204, 315, 426, 537 and 648 °C, respectively. The foregoing discussions illustrate the fact that the radial position of the seal is limited by not only the rotational speed (as discussed earlier) but also by the operating temperature for a desired initial clearance.

Also, as the clearance increases (see Figures 12 to 14), the same trend of *TGR* decreasing with increasing *SCR* continues. Typically, *SCR* range goes up to 0.02, 0.06 and 0.1 for an initial clearance of 0.5, 1.5 and 2.5 mm, respectively, for the chosen range of seal inner radius. Further, it is seen that for the lower

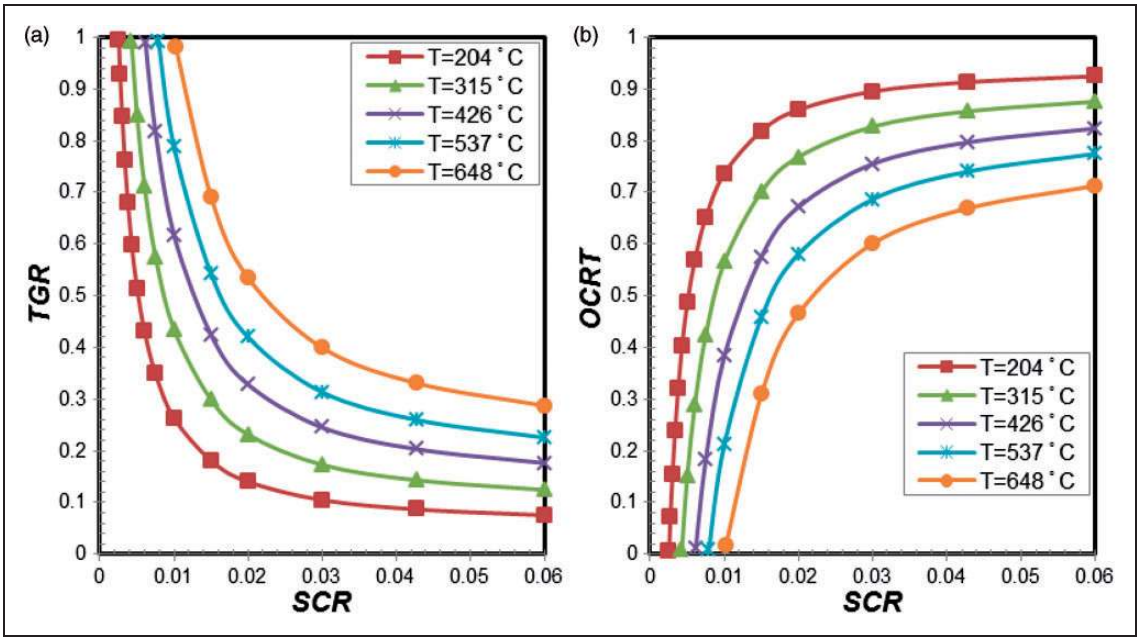

Figure 13. Non-dimensional (a) thermal growth and (b) operating clearance as a function of seal inner radius for an initial clearance of 1.5 mm at different temperature conditions.

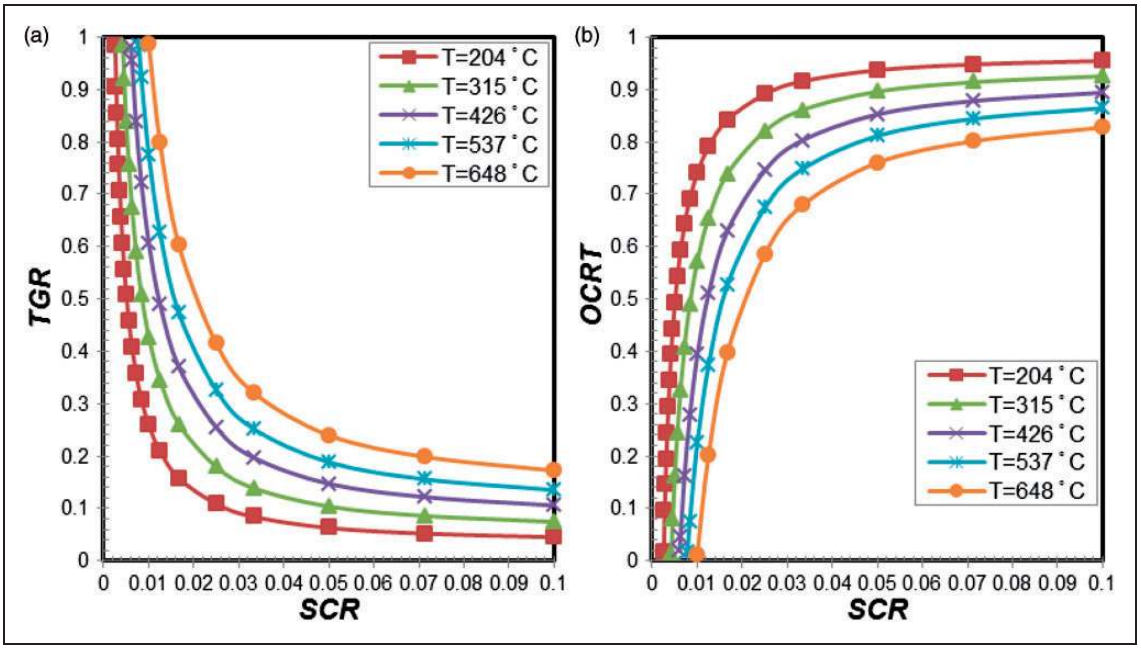

Figure 14. Non-dimensional (a) thermal growth and (b) operating clearance as a function of seal inner radius for an initial clearance of 2.5 mm at different temperature conditions.

bound temperature of 204 °C, the seal inner radius up to 189, 589 mm can be accommodated, respectively, for an initial clearance of 0.5, 1.5 mm; and go beyond 700 mm (up to 980 mm) for an initial clearance of 2.5 mm. For the chosen higher bound temperature of 648 °C, the seal inner radius up to 42, 147 and 250 mm can be accommodated, respectively, for an initial clearance of 0.5, 1.5 and 2.5 mm. This indicates that for larger initial clearance, a broader range of seal inner radii can be accommodated, besides wider operating temperatures. However, the seal initial clearance can be ascertained only after determining the leakage flow rates. The following section discusses the leakage aspects. It may be inferred from Figures 11 to 14 that *TG* is sensitive to the smaller *SCR*, irrespective of the temperature and the influence decreases gradually with the increasing ratio. This implies that the influence of thermal growth on leakage cannot be ignored and it is particularly true for smaller clearances, regardless of temperature. Conversely, the influence is expected to

be less significant when SCR exceeds 0.03, and temperature falls below 204 °C for larger initial clearance of 1.5 and 2.5 mm.

Leakage flow analysis

Figure 15 shows the leakage flow rate as a function of PR and clearance under static condition. In general, the leakage flow increases with PR. However, the trend becomes linear typically once PR reaches 1.7 for higher clearance of 2.5 mm. The start of linearity falls as low as PR reaching 1.3 for lower clearance 0.1 mm. Figure 15 can be used as a quick preliminary design chart for finding the leakage flow rate for a wide ranging PR (1.1–2.5) for any given initial clearance in the range of 0.1–2.5 mm.

The flow domain is updated with the operating clearances, initially with C_1 and finally with C_3 with the appropriate boundary conditions imposed. Adequate care is taken to ensure the new grids generated have greater level of accuracy and reliability, as done earlier. Thus, CFD analysis has been performed with operating clearances by considering (i) the centrifugal growth alone for a rotational speed of 3000 rad/s under ambient condition and (ii) both the centrifugal and thermal growth at the same speed for three temperatures in the range of 200–450 °C. The density and viscosity of air at standard atmospheric pressure for the corresponding temperature conditions are supplied. The choice of operating temperature and rotational speed range depends on net radial growth, which in turn is greatly influenced by disk/shaft radius. To facilitate comparison at different temperatures, the rotational speed has been chosen as 3000 rad/s, as lower speeds have least impact on leakage flow rate (see Figure 4(a)). At this particular speed, the seal can operate up to 450 °C (see Figure 4(b)), safely in order to ensure a net operating clearance (say ~0.1 mm); beyond which potential rubbing may occur for the specified initial clearance of 0.5 mm.

Figure 16 shows the leakage flow rate for the operational clearances at an angular speed of 3000 rad/s for different temperature conditions. It is evident that the leakage flow rate decreases considerably with centrifugal growth and further gets reduced drastically as the thermal growth is included. The radial growth effect on leakage flow rate at varied PR is quantified in terms of percentage reduction in leakage flow rate ($PRLF$) with respect to static condition, which is calculated as

$$PRLF = \frac{M_i - M}{M_i} \times 100 \tag{11}$$

Here M_i represents leakage flow rate for static cold condition (without any growth) and M represents leakage flow rate for the operating clearance condition (considering radial growth) at an angular speed of 3000 rad/s. Figure 17 shows the influence of radial growth on leakage as function of temperature and PR

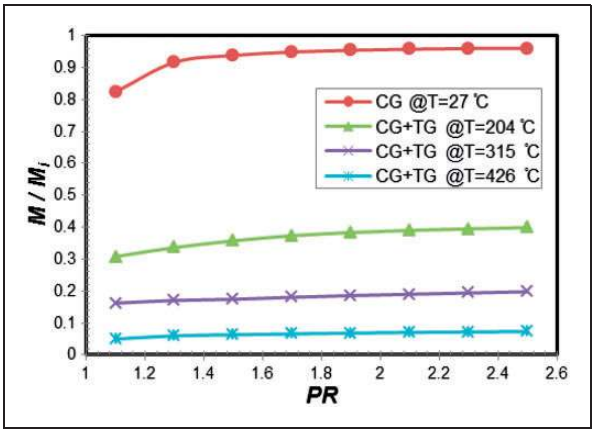

Figure 16. Leakage flow rate for different temperature conditions at $\omega = 3000$ rad/s, incorporating radial growth for seal with $R = 50$ mm and $C = 0.5$ mm.

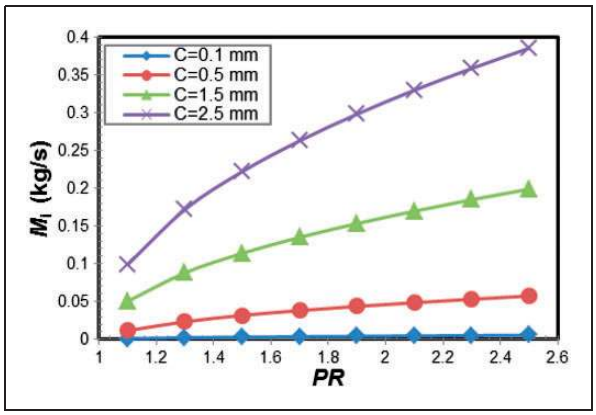

Figure 15. Leakage flow rate as a function of PR and initial clearance for static condition.

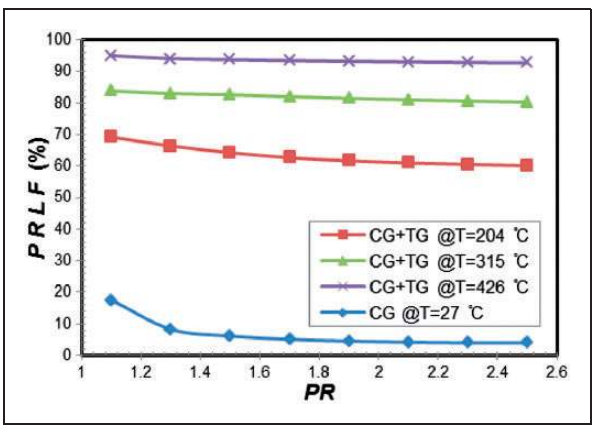

Figure 17. Effect of radial growth on leakage at $\omega = 3000$ rad/s, as function of temperature and PR.

for a rotational speed of 3000 rad/s at various temperature conditions. It is obvious that the leakage flow rate decreases considerably with centrifugal growth at a rotational speed of 3000 rad/s. Typically, the leakage flow rate reduces by 18% for a lower *PR* of 1.1 and 4% for higher *PR* of 2.5. The leakage flow rate reduces drastically as the thermal growth is also included for the corresponding temperature conditions. Further, the *PRLF* value increases with increasing temperature. That is, the higher the temperature, the greater is the reduction in leakage flow rate as reported by Andrés and Ashton.[25] Further, it is interesting to note that the PR has almost negligible influence on *PRLF* at elevated temperatures (say, above 315 °C).

Design guidelines and procedure

This section describes the application of an iterative process involving CFD and FEA techniques and the non-dimensional design variables, which can be used to decide on the choice of initial clearance. In order to prevent rubbing, limiting *CGR* and *OCRC*, based on operating speed or limiting *TGR* and *OCRT*, based on temperature conditions have to be established so that a safe operating clearance (say ~0.1 mm) can be maintained. The combination of different speed and temperature gives a different net radial growth. Further, *TG* and *CG* values are distinctly different not only for different combinations of speed and temperature of seals but also for different locations. Hence the designer has to choose the speed range and temperature range for a particular initial clearance according to the seal location in such a way that the net radial growth ratio (*NRGR*) does not exceed the maximum limit (say ~0.7). Accordingly, the minimum limit for the net operating clearance ratio (*NOCR*) can be chosen as 0.3, so that potential rubbing is avoided during the start-up and shut down (transient) and also to account for the stator thermal deformation approximately, which was presumed to be negligible and not accounted earlier for calculating the operating clearance.

A generic design procedure involving the following seven steps is devised for deciding the initial clearance, systematically.

Step 1: Get initial input, including the seal geometry, inner radius of seal (radial location), material properties, thermal properties and operating conditions.
Step 2: Choose an initial clearance in the range 0.1–2.5 mm judiciously, if not known a priori.
Step 3: Compute *SCR* using equation (1).
Step 4: Obtain *CGR, TGR* (getting *OCRC, OCRT* is optional) from the corresponding non-dimensional charts (for the present case: see Figures 7 to 14), and calculate U_{CG} and U_{TG} using equations (2) and (4).
Step 5: Compute net operating clearance C_3 using equation (7).
Step 6: Check if C_3 is of order ~0.1 mm; if not go back to step 2 and choose a relatively smaller or larger initial clearance, accordingly.
Step 7: Perform CFD analysis with appropriate boundary conditions for the net operating clearance C_3 to predict the leakage flow rate.

It may be noted that the iterative process (step 6) is redundant if the initial clearance is known a priori.

Two numerical examples are given in the following sub-sections to demonstrate the design procedure for the seal considered. However, similar kind of design charts (Figures 7 through 14) can be generated using the same methodology along with the non-dimensional variables for more advanced rotating GT seals. Thus, the design procedure can be adopted for the estimation of radial growth, operating clearances and subsequently to predict the leakage flow rate of a rotating GT seal.

Numerical example 1: Pre-determine the radial growth, operating clearance and leakage flow rate

Estimate the radial growth and operating clearance of a GT seal (configuration as shown in Figure 1) for the following data: seal inner radius = 50 mm, tooth height = 10.5 mm, initial clearance = 0.5 mm; seal to be mounted on a solid disk and operating at a speed of 3000 rad/s and temperature 426 C. Assume stator deformation is negligible. Also predict the leakage flow rate at a PR of 1.5 for the given operating conditions. Assume both disk and seal are made of INCONEL 718.

Solution: Firstly, *SCR* is calculated as 0.01, using equation (1). Secondly, from Figure 8(a), *CGR* is obtained as 0.029 for the given speed, which corresponds to a centrifugal growth of 14 μm. Thirdly, from Figure 12(a), *TGR* can be obtained as 0.704, which corresponds to a thermal growth of 352 μm. Thus, the combined radial growth is 366 μm. After the net radial growth is estimated, net operating clearance C_3 is calculated as 0.1335 mm, using equation (7). Subsequently, a CFD analysis with appropriate boundary conditions is performed to arrive at the leakage flow rate as 0.00199 kg/s (see Figures 15 and 16).

Numerical example 2: Choose an optimum initial clearance and predict leakage flow rate

Design the GT seal (configuration as shown in Figure 1) for an optimum initial clearance for the following data: seal located at a radial distance of 100 mm from the shaft axis, tooth height = 10.5 mm;

seal to be mounted on a solid disk and operating at a speed of 1000 rad/s and temperature 205 °C. Assume both disk and seal are made of INCONEL 718.

Solution: Firstly, choosing 0.1 mm as initial clearance, and using equation (1), *SCR* is calculated as 0.001. However, choosing 0.1 mm as initial clearance is practically not possible as *TGR* value exceeds 1, as seen from Figure 11(a). Secondly, choosing an initial clearance of 0.5 mm, *SCR* is calculated as 0.005 for which *CGR* is 0.0161 (Figure 8(a)) and the corresponding *CG* value is 8 μm. For the same *SCR*, *TGR* is 0.544 (Figure 11 (a)) and the corresponding *TG* value is 272 μm. Equation (7) gives C_3 as 0.2 mm. Thus, the initial clearance of 0.5 mm can be considered as the near optimum initial clearance, for which the operating clearance is 0.2 mm. A few iterative processes are required to arrive at an optimum initial clearance, so that a safe operating clearance (say ~0.1 mm) can be maintained. Finally, a CFD analysis with appropriate boundary conditions has to be performed for the net operating clearance to arrive at the leakage flow rate for the desired range of *PR*, which is not reported here for the sake of brevity.

In a similar manner, the range of operating speed (maximum limiting speed) and temperature (maximum limiting temperature) conditions could also be explored for a particular seal inner radius so that an optimum initial clearance can be selected before the seal is placed. Also an appropriate interpolation technique can be used for getting any intermediate values depending on the level of accuracy.

The major limitation of the present work is that the margin of uncertainty cannot be ascertained because benchmark data are not available in the literature. The uncertainty may enter into the result due to the effect of the overall length of the seal (L/R ratio), type of seal (e.g. stepped, inclined, etc.), the mechanism of heat transfer between the fluid and the seal, stator growth and the like. Further studies into benchmark experiments varying the above are required to ascertain the uncertainty.

Conclusions

A generic design procedure has been developed and demonstrated, perhaps for the first time, which will allow GT designers to estimate numerically the initial clearance and the leakage flow rate for rotating GT seals used in a secondary air system. The basis for the design is to prevent the onset of seal rubbing that might arise due to centrifugal and thermal growth. The design guidelines have been formulated through extensive parametric studies and non-dimensionalization.

The key findings from the present study as applicable to a six-tooth straight-through rotating labyrinth GT seal under representative operating conditions are summarized below:

1. The centrifugal growth (*CG*) varies as a quadratic function with rotational speed. On the other hand, thermal growth (*TG*) varies almost linearly with temperature. Further, *TG* values are of one order of magnitude higher than *CG* values for the chosen range of operating conditions.
2. The seven non-dimensional design variables relating to seal clearance, centrifugal growth, thermal growth and operating clearances (*SCR, CGR*, *OCRC*, *TGR, OCRT, NRGR* and *NOCR*) are found to be beneficial in generalizing the radial growth of seals and determination of operating clearance during preliminary design stages of a seal. Further, they provide an insight on the operating speed and temperature limits for seals placed at different radial locations and aid in arriving at an initial clearance judiciously.
3. The maximum limiting rotational speed and temperature is confined by not only seal radial location but also the desired initial clearance. The larger the initial clearance, the broader is the range of radial location covered, besides a wider operating condition.
4. The centrifugal growth of seal is more prominent for smaller clearance and higher rotational speed combinations. The influence of *CG* on leakage is anticipated to be insignificant as *SCR* exceeds 0.004, 0.01, 0.02 and 0.025, respectively, for a constant initial clearance of 0.1, 0.5, 1.5 and 2.5 mm.
5. The thermal growth of seal is considerably large for smaller SCRs below 0.04 and temperatures above 204 °C. Thus, the influence of *TG* on leakage is anticipated to be less significant at SCRs above 0.04 and temperatures below 204 °C.
6. The PR has negligible influence on leakage at elevated temperatures. However, it has a considerable effect on leakage for temperatures less than or equal to 204 °C and the most significant influence is observed at lower to mid-range *PR* (say 1.1–1.7). Thus, the initial clearance can be decided based on the operating temperature relative to cold condition, except at low pressure and high speed combinations.

The demonstrated methodology can also be extended further for different classes of rotating seals with more complex configuration (e.g. stepped rotating seal) and arbitrary tooth profile (e.g. inclined seal). Subsequently, the proposed methodology may perhaps aid the designer in arriving at an optimum initial clearance and leakage flow rate for any rotating seal of interest, ensuring an effective and reliable sealing, thereby avoiding fatal damage to the GT engine.

Acknowledgements

The authors express their profound gratitude to CFD Centre and High Performance Computing Facility, IIT Madras for the computational support, and Gas Turbine Research Establishment (GTRE), Bangalore for the generous technical support. We are grateful to Prof. E. G. Tulapurkara, Department of Aerospace Engineering, IIT Madras for his valuable time and comments on the manuscript.

Conflict of interest

None declared.

Funding

This research received no specific grant from any funding agency in the public, commercial, or not-for-profit sectors.

References

1. Aslan-zada FE, Mammadov VA and Dohnal F. Brush seals and labyrinth seals in gas turbine applications. *Proc IMechE Part A: J Power and Energy* 2013; 227: 216–230.
2. Sneck HJ. Labyrinth seal literature survey. *J Lubricat Technol* 1974; 96: 579–581.
3. Hwang M, Pope AN and Shucktis B. Advanced seals for engine secondary flow path. *AIAA J Propul Power* 1996; 12: 794–799.
4. Childs DW and Vance JM. Annular gas seals and rotordynamics of compressors and turbines. In: *Proceedings of 26th turbomachinery symposium*, Texas, USA, 1997, pp.201–220. College Station, Texas: Turbomachinery Laboratory, Texas A&M University.
5. Tiwari R, Manikandan S and Dwivedy SK. A review of the experimental estimation of the rotor dynamic parameters of seal. *Shock Vibr Digest* 2005; 37: 261–284.
6. Chupp RE, Hendricks RC, Lattime SB, et al. Sealing in turbomachinery. *AIAA J Propul Power* 2006; 22: 313–349.
7. Chew JW and Hills NJ. Computational fluid dynamics for turbomachinery internal air systems. *Phil Trans R Soc A Math Phys Eng Sci* 2007; 365: 2587–2611.
8. Gamal AM, Ertas BH and Vance JM. High-pressure pocket damper seals: leakage rates and cavity pressures. *ASME J Turbomach* 2007; 129: 826–834.
9. Ashton Z. *High temperature leakage performance of a hybrid brush seal compared to a standard brush seal and a labyrinth seal*. MS Thesis, Texas A&M University, USA, 2009.
10. Li Z, Li J, Yan X, et al. Numerical investigations on the leakage flow characteristics of pocket damper labyrinth seals. *Proc IMechE Part A: J Power and Energy* 2012; 226: 932–948.
11. Subramanian S, Sekhar AS and Prasad BVSSS. Performance analysis of a rotating labyrinth seal with radial growth. In: *Proceedings of ASME Turbo Expo 2013*, San Antonia, Texas, USA, 3–7 June 2013; paper no. GT2013-95708. New York: ASME.
12. Anderson A. *Gas seal leakage at high temperature: a labyrinth seal and an all-metal compliant seal of similar clearance*. MS Thesis, Texas A&M University, USA, 2013.
13. Qiu B, Li J and Yan X. Investigation into the flow behaviour of multi-stage brush seals. *Proc IMechE Part A: J Power and Energy* 2014; 228: 416–428.
14. Li J, Qiu B and Feng Z. Experimental and numerical investigations on the leakage flow characteristics of the labyrinth brush seal. *ASME J Eng Gas Turbines Power* 2012; 134: 102509.
15. Alexiou A and Mathioudakis K. Secondary air system component modeling for engine performance simulations. *ASME J Eng Gas Turbines Power* 2009; 131: 031202.
16. Amirante D, Hills NJ and Barnes CJ. Use of dynamic meshes for transient metal temperature prediction. In: *Proceedings of ASME Turbo Expo 2012*, Copenhagen, Denmark, San Antonia, USA, 11–15 June 2012; paper no. GT2012-68782. New York: ASME.
17. Ganine V, Javiya U, Hills NJ, et al. Coupled fluid-structure transient thermal analysis of a gas turbine internal air system with multiple cavities. *ASME J Eng Gas Turbines Power* 2012; 134: 102508.
18. ANSYS Mechanical 14, ANSYS Users Guide, Element Description, 2011.
19. www.specialmetals.com/documents/Inconelalloy718.pdf (accessed 16 July 2012).
20. Timoshenko S and Goodier J. *Theory of elasticity*. New York: McGraw-Hill Book Company, 1970.
21. Melcher KM and Kypuros JA. Toward a fast-response active turbine tip clearance control. In: *Sixteenth international symposium on air breathing engines 2003*, Cleveland, Ohio, USA, 31 August–5 September, 2003; paper no. ISABE 2003-1102. Reston, Virginia: AIAA.
22. Kim TS and Cha KS. Comparative analysis of the influence of labyrinth seal configuration on leakage behaviour. *J Mech Sci Technol* 2009; 23: 2830–2838.
23. Wittig S, Schelling U, Kim S, et al. Numerical predictions and measurements of discharge coefficients in labyrinth seals. In: *ASME 32nd international gas turbine conference and exhibition*, Anaheim, CA, 1987; paper no. GT1987-188. New York: ASME.
24. Hirano T, Guo Z and Kirk RG. Application of computational fluid dynamics analysis for rotating machinery – Part II: labyrinth seal analysis. *ASME J Eng Gas Turbines Power* 2005; 127: 820–826.
25. Andrés LS and Ashton Z. Comparison of leakage performance in three types of gas annular seals operating at a high temperature (300 °C). *Tribol Trans* 2010; 53: 463–471.

Appendix

Abbreviation

CFD	Computational Fluid Dynamics
CG	centrifugal growth of seal
CGR	Centrifugal Growth Ratio
FEA	Finite Element Analysis
GT	Gas Turbine
OCRC	Operating Clearance Ratio due to Centrifugal growth
OCRT	Operating Clearance Ratio due to Thermal growth
PR	Pressure Ratio
PRLF	Percentage Reduction in Leakage Flow rate

RANS	Reynolds Averaged Navier-Stokes Equations
TG	thermal growth of seal
$NOCR$	Net Operating Clearance Ratio
$NRGR$	Net Radial Growth Ratio
SCR	Seal Clearance Ratio
TGR	Thermal Growth Ratio

Notation

b	width of the seal tooth (mm)
C	initial clearance (mm)
C_1	operating clearance due to CG alone (mm)
C_2	operating clearance due to TG alone (mm)
C_3	net operating clearance due to combined CG and TG (mm)
CD	coefficient of discharge
E	modulus of elasticity of the rotor material (GPa)
h	height of the seal tooth (mm)
L	length of the seal (mm)
M_i	leakage flow rate for initial clearance (static cold condition) (kg/s)
M	leakage flow rate for operational clearance (considering radial growth) (kg/s)
n	number of teeth
N	number of nodes in FEA
p	pitch of the seal tooth (mm)
r	radius of rotor (also outer radius of seal) (mm); $r = R + h$
R	radius of the shaft (also inner radius of seal) (mm)
T	air temperature (°C)
T_{ref}	reference temperature of rotor (°C)
T_s	surface temperature of rotor (°C)
U_{CG}	radial deformation due to CG (mm)
U_{TG}	radial deformation due to TG (mm)
α	thermal expansion coefficient for rotor material (1/°C)
ν	Poisson's ratio of the rotor material
ρ	density of the rotor material (kg/mm^3)
ω	angular speed of the rotor (rad/s)